Computing Eddy Currents in Induction Melting Processes

Ştefan Nagy*, Adrian Nagy* and Dorelu Dragoş Betea*
*Department of E.M.U.E.E,
University of Oradea, Faculty Electrical Engineering and Information Technology,
1 Universității street, 410087 Oradea, Romania, E-Mail: snagy@uoradea.ro

***Abstract* – This paper presents the eddy currents distribution in the melting process of non-ferrous alloys. The obtained results offer us some valuable information about the melting of non-ferrous alloys and about ways of optimizing the electro-technique equipment design for induction heating machines. This paper also presents a method to determine the evolution of the solidification layer in controlled casting techniques**

***Keywords:* induction heating, eddy currents**

I. INTRODUCTION

The computation of the losses due to eddy current is a problem of great technical interest. Most of the time these losses are not desired and designers try to reduce them. Other times these losses are useful because of their heating effect, allowing the heating of certain parts of a conductor. To determine the losses due to eddy currents involves the computation of the electromagnetic field in conductors, thus solving complicated quasi-stationary regime problems, [1, 4, 5, 6].

The literature presents different approaches to determine the electromagnetic field in quasi-stationary regime, in linear and non-linear conductors, immobile mediums, 2D structures, [2]. Given the great development of computational power, researchers focus on developing some algorithms to solve numerically the eddy currents problem in 3D structures, [3].

II. EDDY CURRENTS DISTRIBUTION

Let us consider the geometry depicted in Fig. 1. It contains a conducting domain Ω_c surrounded by an unbounded non-conducting domain Ω_0 (e.g. air). The current sources (coils) are situated here. Let us denote by $\partial\Omega_c$ the surface bordering the conducting material and by $\partial\Omega_0$ the outer boundary. In the free space region Ω_0 the following Maxwell equations are valid in the quasi-stationary limit:

$$\begin{aligned} &\nabla \times \mathbf{H} = \mathbf{J}_0 \\ &\nabla \cdot \mathbf{B} = 0. \\ &\mathbf{B} = \mu\mathbf{H} \ \ or \ \ \mathbf{B} = f(\mathbf{H}) \end{aligned} \tag{1}$$

where $\mathbf{J}_0$ represent the impressed current sources.

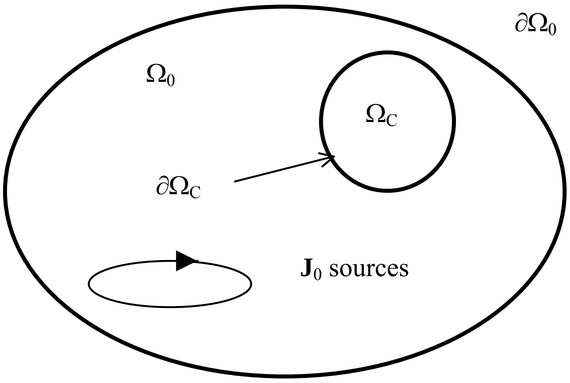

Fig.1. Domain configuration for eddy current problems

In the conducting domain we have:

$$\begin{aligned} &\nabla \times \mathbf{H} = \mathbf{J} \\ &\nabla \cdot \mathbf{B} = 0. \\ &\mathbf{B} = \mu\mathbf{H} \ \ or \ \ \mathbf{B} = f(\mathbf{H}) \\ &\nabla \times \mathbf{E} = -\frac{\partial \mathbf{B}}{\partial t} \\ &\mathbf{J} = \sigma\mathbf{E} \end{aligned} \tag{2}$$

where $\mathbf{J}$ is the density of the induced eddy currents. On the outer border $\partial\Omega_0$ typically two types of conditions may be encountered:

$$\begin{aligned} &\mathbf{B} \cdot \mathbf{n} = 0 \quad on \ \ \partial\Omega_B \\ &\mathbf{H} \times \mathbf{n} = 0 \ \ on \ \ \partial\Omega_H \end{aligned} \tag{3}$$

on the condition that $\partial\Omega_B \cup \partial\Omega_H = \partial\Omega_0$. These are called longitudinal boundary conditions. If $\partial\Omega_H$ consist of *n* non-overlapping surfaces in order to ensure the uniqueness of the field problem on *n-1* the magnetic fluxes have to be given:

$$\int_{S_i} \mathbf{B} \cdot \mathbf{n} = \phi_i \quad \bigcup_{i=1}^{n} S_i = \partial\Omega_H \tag{4}$$

On the $\partial\Omega_C$ interface the following continuity conditions are to be imposed:

$$\begin{aligned} &\mathbf{B}_C \cdot \mathbf{n} = \mathbf{B}_0 \cdot \mathbf{n} \\ &\mathbf{H}_C \times \mathbf{n} = \mathbf{H}_0 \times \mathbf{n} \end{aligned} \tag{5}$$

where subscript C denote conducting region and 0 air region.

Usually a potential solution to the problem is preferred. In the following we refer to the *A, V –* ψ one [3]. This means using magnetic vector potential in Ω_C together with scalar electric potential combined with the use of magnetic scalar potential in the non-conducting area.

In Ω_C the use of potentials A and V yields the following second order equation:

$$\nabla \times \nu \nabla \times \mathbf{A} + \sigma \frac{\partial \mathbf{A}}{\partial t} + \sigma \nabla V = 0 \tag{6}$$

which includes also the divergence free condition verified by the induced eddy currents J ($\nu = \mu^{-1}$). To obtain a significant reduction of computing effort in $\Omega 0$ we use the following decomposition:

$$\mathbf{H} = \mathbf{H}_0 - \nabla \phi \tag{7}$$

where H_0 is the field due to source currents and can be easily computed by Biot-Savart-Laplace relation. ϕ is reduced magnetic scalar potential. We restrict the use of ϕ to only the sources region. In the source free regions of Ω_0 in order to avoid some cancellation of errors we use:

$$\mathbf{H} = -\nabla \psi \tag{8}$$

where ψ is total scalar magnetic potential. Consequently in Ω_0 the second order equation is given by:

$$\nabla \cdot \mu \nabla \psi = 0 \tag{9}$$

The outer boundary conditions became now:

$$\mathbf{n} \cdot \mu \nabla \psi = 0 \quad on \quad \partial \Omega_B$$
$$\psi = 0 \quad on \quad \partial \Omega_H \tag{10}$$

whilst the interface boundary conditions can be written as:

$$\mathbf{n} \cdot \nabla \times \mathbf{A} - \mathbf{n} \cdot \mu \nabla \psi = 0$$
$$\nu \nabla \times \mathbf{A} \times \mathbf{n} - \nabla \psi \times \mathbf{n} = 0 \tag{11}$$

The fact that the eddy currents cannot flow across $\partial \Omega_c$ the boundary amounts to imposing on $\partial \Omega_c$ the following:

$$\mathbf{n} \cdot \left(-\sigma \frac{\partial \mathbf{A}}{\partial t} - \sigma \nabla \mathrm{V} \right) = 0 \tag{12}$$

If conductivity is constant in domain Ω_c it can be shown [3] that scalar potential V is constant in Ω_c and hence it can be chosen to be zero. Thus (12) becomes unnecessary. Hence A becomes in fact a modified vector potential [3].

III. EXPERIMENTAL RESULTS

The computations for the eddy currents, for the melting process of a siliminum alloy, were made using a 125 kg capacity melting furnace. The heating process from 20° to 690° takes about 2158 sec. The module used for the numerical modeling of the heating process is "Magneto-Thermal". This software automatically couples the magneto-dynamic module with the transitory thermal module.

Fig. 2 presents the experimental model that we used, which has the following components: non-ferrous molten, siluminum (1), crucible (2), coils of the inductor (3), thermal insulating material, fire clay (4), insulting material, asbestos (5) and fireproof concrete (6).

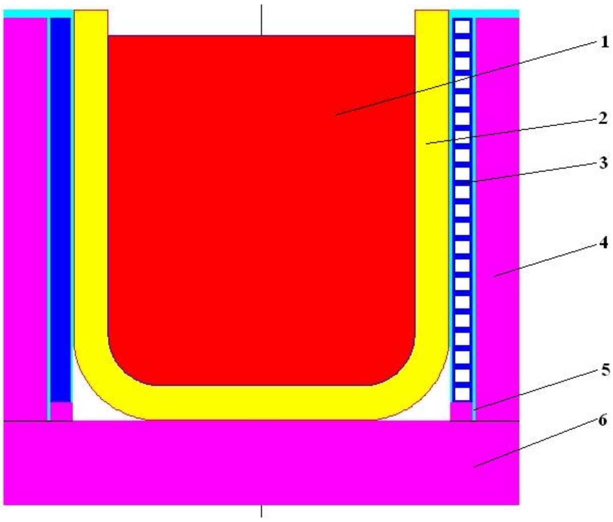

Fig.2. The experimental model.

Fig. 3 presents the current density at the beginning of the melting process t ≅ 5 sec.

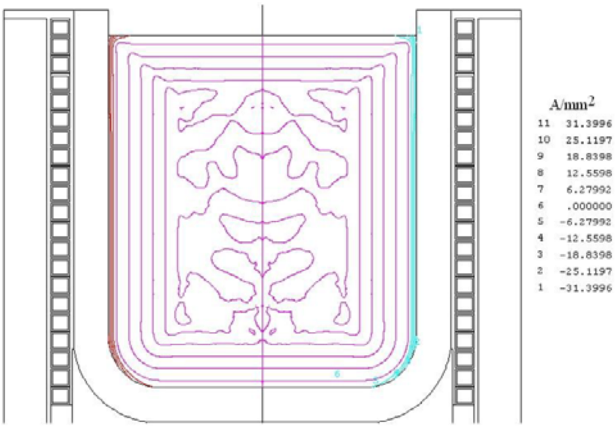

Fig. 3. Current density at t ≅ 5 sec.

Fig. 4 presents the current density during the melting process t ≅ 1100 sec.

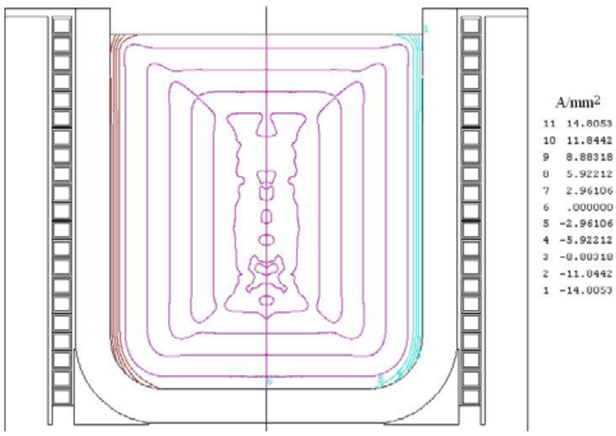

Fig. 4. Current density at t ≅ 1100 sec.

Fig. 5 presents the current density at the end of the melting process t ≅ 2200 sec.

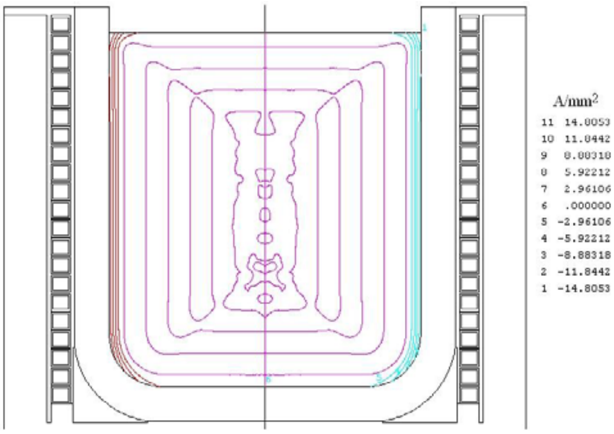

Fig. 5. Current density at t ≅ 2200 sec.

The variation of the power density at the beginning of the process, t ≅ 5 sec, is presented in Fig. 6.

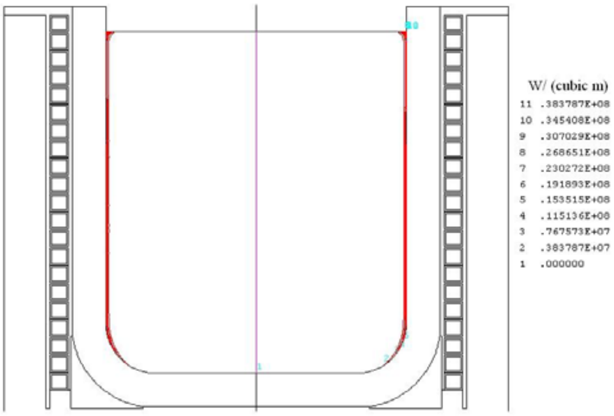

Fig. 6. Power density variation at t ≅ 5 sec.

Fig. 7 presents the variation of the power density during the melting process t ≅ 1100 sec.

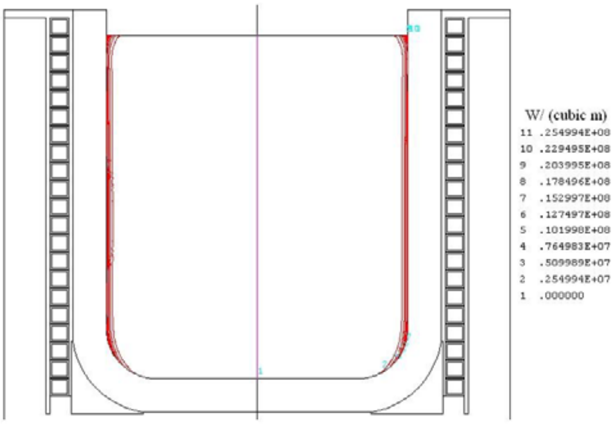

Fig. 7. Power density variation at t ≅ 1100 sec.

The variation of the power density at the end of the process, t ≅ 2200 sec, is presented in Fig. 8.

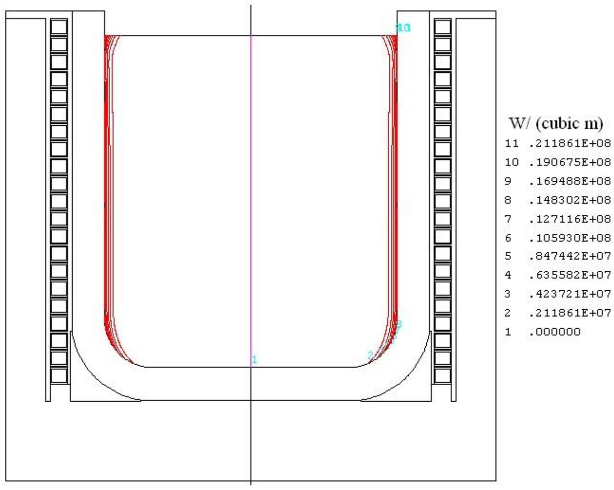

Fig. 8. Power density variation at t ≅ 2200 sec.

Fig. 9 presents the magnetic field intensity at the beginning of the melting process t ≅ 5 sec.

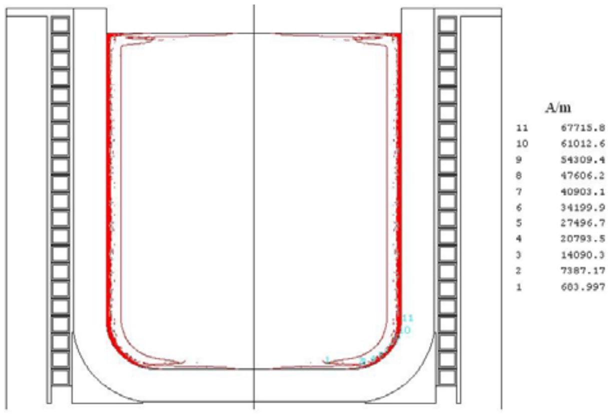

Fig. 9. Magnetic field intensity at t ≅ 5 sec.

Fig. 10 presents the magnetic field intensity during the melting process t ≅ 1100 sec.

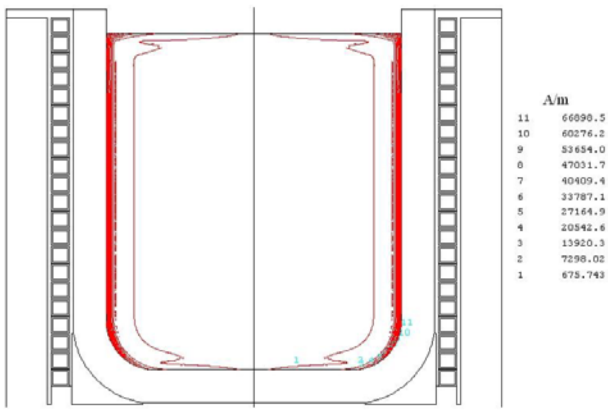

Fig. 10. Magnetic field intensity at t ≅ 1100 sec.

Fig. 11 presents the magnetic field intensity at the end of the melting process t ≅ 2200 sec.

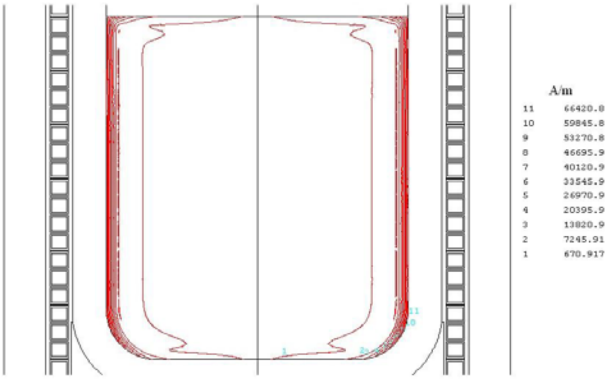

Fig. 11. Magnetic field intensity at t ≅ 2200 sec.

IV. CONCLUSIONS

As analytical methods don't provide precise solutions, the utilization of numerical methods that allow the solving of problems with hundreds of unknowns in discrete representation is imposed.

The accurate knowledge of electromagnetic phenomena in the case of induction heating as well as the distribution of thermal field allows the analysis and the optimal design of electro-thermal equipment. The obtained results offer us some valuable information about the melting of non-ferrous alloys and about ways of optimizing the electro-technique equipment design for induction heating machines.

The knowledge of electromagnetic and thermal fields in a heating process allows the access to the computation of global performances in transient or permanent regime.

REFERENCES

[1] T. Maghiar, T. Leuca, F. I. Hantila, "*Numerical analysis of eddy current heating*", Editura Universitatii din Oradea, Oradea, 2001.

[2] O. Biro, K. Preis, "*Finite element analysis of eddy currents*", IEEE Trans. on Magn., No. 2, pp 414 – 423, 1990.

[3] R. Albanese, F. I. Hantila, G. Preda, G. Rubinacci, "*A nonlinear eddy current integral formulation for moving bodies*", IEEE Trans. on Magn., No. 2, pp 2529-2534, 1998.

[4] Şt. Nagy, T. Maghiar, C. Molnar, "*Numerical analysis of Eddy curents and thermal field within the heating of noferrous alloys*", IGTE Symposiun, Graz - Austria, pp. 32-35. 11-13 September 2000.

[5] T. Maghiar, Şt. Nagy, I.F. Hănţilă, A. Nagy, "*The evolution of the hardening surface in the controlled casting process*", The 10th International IGTE Symposium on Numerical Field Calculationn in Electrica Engineering, Graz-Austria, pp. 290-294, 16-18 September 2002.

[6] Şt. Nagy, T. Maghiar, "*Numerical analysis of melting of non-ferrous alloys*", International Conference ELEKTROENERGETIKA 2001, Stara Lesna – Slovakia, pp. 181-185, 22-23 January 2001.